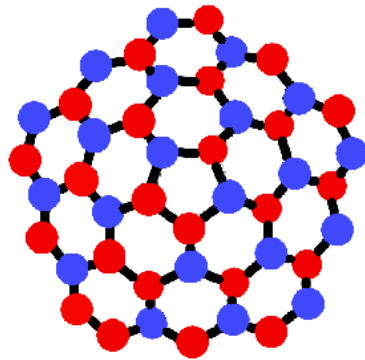

Effect of Topology on The Critical Charge in Graphene



Baishali Chakraborty¹, Kumar S.Gupta¹ and Sidhdhartha Sen²

¹Theory Division, Saha Institute of Nuclear Physics
1/AF Bidhannagar, Calcutta 700064

²Trinity College, Dublin, Ireland

(Ref: [arXiv:1010.5873v1](https://arxiv.org/abs/1010.5873v1)[cond-mat.mes-hall])

Introduction

- Graphene is the first example of a truly two dimensional crystal.
- It was experimentally discovered in 2004 when a group of physicists from Manchester University, led by Geim and Novoselov, extracted a single sheet (a monolayer of atoms) of graphene from graphite by the micromechanical cleavage technique.

Introduction

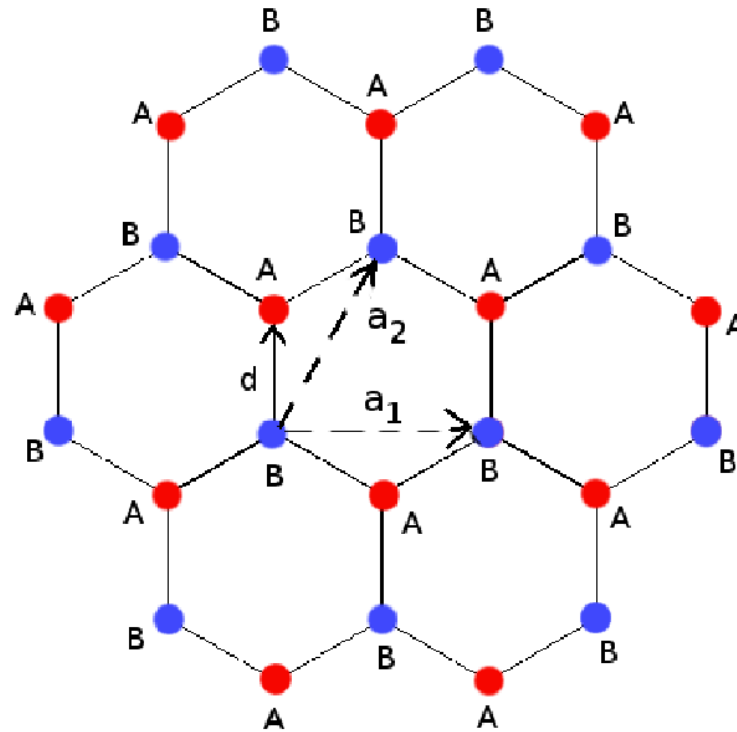


Figure 1: Lattice structure of graphene

Introduction

- Graphene has a planer hexagonal honeycomb lattice structure as shown in the figure.
- The hexagonal lattice is made of two triangular sublattices. The lattice sites are denoted by type A and type B.
- The reciprocal lattice is hexagonal. Among its six vertices only two are inequivalent corresponding to the two sublattices A and B. These two points are known as Dirac points.

Introduction

- Low energy Dirac excitations of a two dimensional gapless graphene sample behave like electrons with the Fermi velocity $v_F \approx 10^6 m/s$.
- Due to a small external charge impurity $Ze \sim 1$, effective Coulomb interaction strength in the sample is given by $\alpha = \frac{Ze^2}{\hbar\kappa v_F} \sim 1$, where the dielectric constant $\kappa \sim 5$.
- When the effective strength of the external charge exceeds a certain critical value α_c , the low energy excitations can form quasi-bound states.
- A nontrivial topology, manifesting itself in the form of nontrivial holonomies for the pseudoparticle wavefunctions, affects this critical charge α_c and the corresponding strong field QED effects in the graphene sample.

Plan of the work

- We Consider a conical topology where an electric charge localized at the apex of the graphene cone can be equivalently described by a suitable combination of electric charge and magnetic flux tube.
- The critical charge α_c depends on the angle of the cone and for a certain value of the angle of the cone, the critical charge is zero.
- The conical topology also affect the scattering phase shifts, quasi-bound state energies and local density of states (LDOS) in graphene.

The Dirac Spinor

- The low energy properties of the quasiparticle states near the Fermi points in graphene can be described by the four component Dirac wave function

$$\Psi = \begin{pmatrix} \Psi_A \\ \Psi_B \end{pmatrix}, \text{ where } \Psi_A = \begin{pmatrix} \Psi_{A+} \\ \Psi_{A-} \end{pmatrix} \text{ and } \Psi_B = \begin{pmatrix} \Psi_{B+} \\ \Psi_{B-} \end{pmatrix}$$

- The pseudospin indices A and B label the two sublattices of the primitive cell of graphene and the valley indices $+$ and $-$ label the two inequivalent Dirac points \mathbf{K}_+ and \mathbf{K}_- respectively.

Dirac equation for planar graphene with a Coulomb charge

- The Dirac equation for the gapless excitations of planar graphene in the presence of a Coulomb charge Ze around the Dirac point K_+ is given by

$$\left[-i\hbar v_F (\sigma_1 \partial_x + \sigma_2 \partial_y) + \sigma_0 \left(\frac{-\alpha}{r} \right) \right] \Psi = E \Psi, \quad (2)$$

where r is the radial coordinate in the two dimensional $x - y$ plane. The Pauli matrices $\sigma_{1,2,3}$ and the identity matrix σ_0 act on the pseudospin indices A, B .

Energy spectrum of Planar Graphene

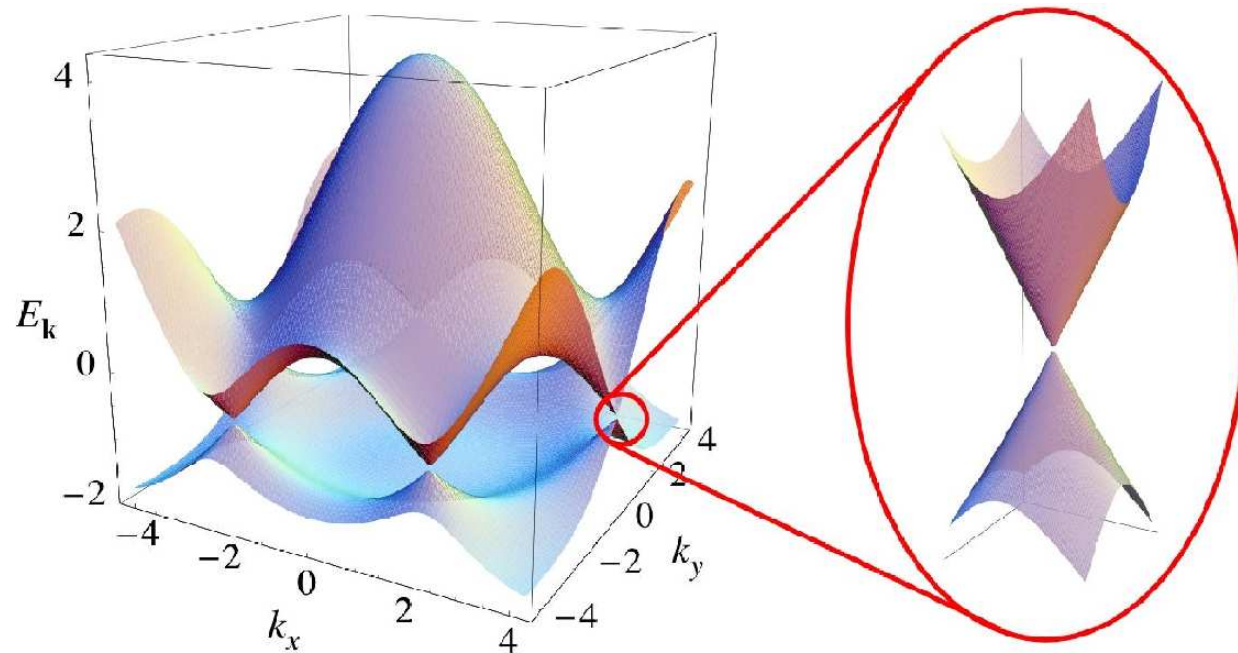


Figure 2: Energy spectrum of planar graphene(Ref:A. H. Castro Neto, F. Guinea, N. M. R. Peres, K. S. Novoselov, A. K. Geim, Rev. Mod. Phys. 81, 109 (2009))

Formation of Cone from Planar Graphene

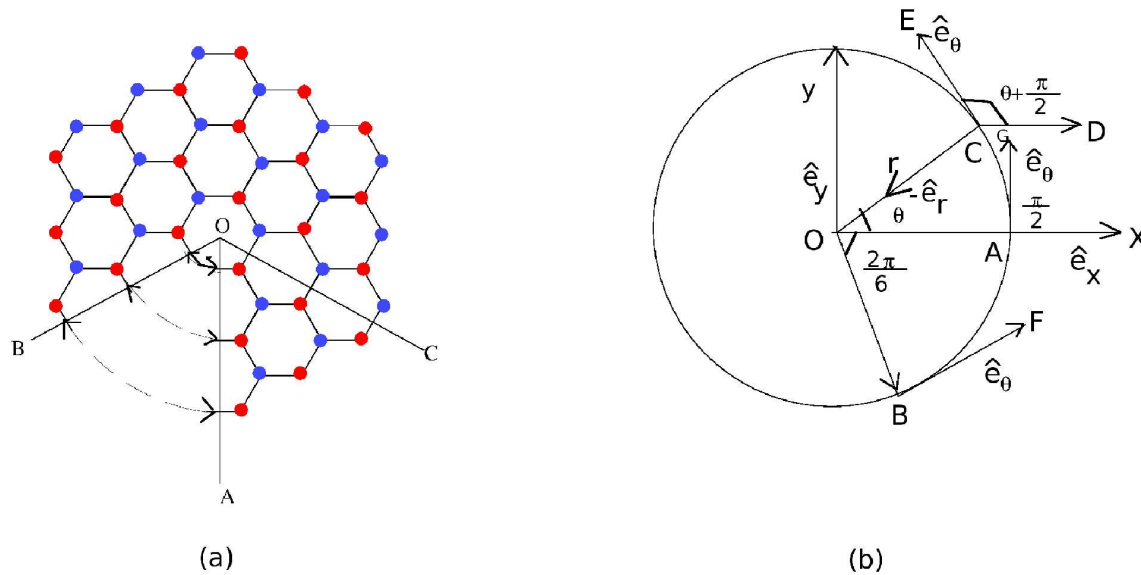


Figure 3: (a) Formation of a cone from plane graphene sheet by cut and paste procedure and (b) Rotation of the coordinate frame due to its new orientation. In Fig. (a) blue atoms represent sublattice A and red atoms represent sublattice B.

Holonomy Modelled Through a Magnetic Flux Tube

- When a cone is formed from a plane graphene sheet by removing n number of sectors, the angular boundary condition obeyed by the Dirac spinor is given by

$$\Psi(\mathbf{r}, \theta = 2\pi) = -e^{i2\pi[\pm\frac{n}{4} + (1-\frac{n}{6})\frac{\sigma_3}{2}]} \Psi(\mathbf{r}, \theta = 0). \quad (3)$$

- The effect of the angular boundary condition (3) on the wave function can be equivalently described by introducing a magnetic flux tube passing through the apex of the cone. The presence of a magnetic vector potential modifies the boundary condition on a Dirac spinor as

$$\Psi(\mathbf{r}, \theta = 2\pi) = -e^{ie2\pi r(1-\frac{n}{6})A_\theta} \Psi(\mathbf{r}, \theta = 0). \quad (4)$$

- Assuming A_θ to be independent of the angle θ .
-

Dirac equation for a graphene cone with a Coulomb charge

- Comparing equation (3) and equation (4) we get

$$A_\theta = \frac{1}{er} \left[\pm \frac{\frac{n}{4}}{\left(1 - \frac{n}{6}\right)} + \frac{\sigma_3}{2} \right]. \quad (5)$$

- Thus the Dirac equation (2) can be written as

$$\left(\begin{array}{cc} -\frac{\alpha}{r} & \partial_r - \frac{i}{r\left(1 - \frac{n}{6}\right)} \partial_\theta \pm \frac{\frac{n}{4}}{r\left(1 - \frac{n}{6}\right)} + \frac{1}{2r} \\ -\partial_r - \frac{i}{r\left(1 - \frac{n}{6}\right)} \partial_\theta \pm \frac{\frac{n}{4}}{r\left(1 - \frac{n}{6}\right)} - \frac{1}{2r} & -\frac{\alpha}{r} \end{array} \right) \Psi = E\Psi \quad (6)$$

Short Distance Behaviour of the Dirac Spinor

- We use an ansatz for the wavefunction given by

$$\Psi(r, \theta) = \sum_j \begin{pmatrix} \Psi_A^{(j)}(r) \\ i\Psi_B^{(j)}(r) \end{pmatrix} e^{-iEr} r^{\gamma - \frac{1}{2}} e^{ij\theta}, \quad (7)$$

where the total angular momentum j takes all half integer values.

- Substituting (7) in (6), we note that the leading short distance behaviour of the wavefunction is given by

$$\Psi_{A,B}^{(j)}(r) \sim r^{\gamma - \frac{1}{2}} \text{ where } \gamma = \sqrt{\nu^2 - \alpha^2} \text{ and } \nu = \frac{(j \pm \frac{n}{4})}{(1 - \frac{n}{6})}. \quad (8)$$

Critical Charge

- From (8) it follows that when $|\alpha|$ exceeds $|\nu|$, γ becomes imaginary.
- The critical value of the coupling is denoted by α_c and it is given by the minimum allowed value of $|\nu|$.
- The parameter ν depends on j and the number of sectors n removed from a plane to form the graphene cone. Hence we see that the critical coupling α_c explicitly depends on the angle of the graphene cone.

Dependence of Critical Charge on Conical Topology

Table 1: The values of critical charge α_c i.e the minimum values of $|\nu|$ for different values of opening angle of the graphene cone i.e for different values of n .

value of n	Critical charge (α_c)	Corresponding (j)
0	0.5	$\pm\frac{1}{2}$
1	0.3	$\pm\frac{1}{2}$
2	0	$\pm\frac{1}{2}$
3	0.5	$\pm\frac{1}{2}$
4	1.5	$\pm\frac{1}{2}$
5	1.5	$\pm\frac{3}{2}$

Scattering Matrix

- Using the zigzag edge boundary condition $\Psi_B^{(j)}(a_0) = 0$, where a_0 is a distance from the apex, of the order of the lattice scale in graphene we obtain the scattering matrix S as

$$S = e^{2i\delta_\nu(k)} = \left[\frac{f_{\alpha,\lambda} + e^{2i\zeta(k)} e^{-\pi\lambda} \mu f_{\alpha,-\lambda}}{e^{\pi\lambda} \mu f_{\alpha,-\lambda}^* + e^{2i\zeta(k)} f_{\alpha,\lambda}^*} \right] e^{-2i\alpha \ln(2kr)} \quad (9)$$

where

- $k = -E$, $\lambda = \sqrt{\alpha^2 - \nu^2}$ and $\mu = \sqrt{\frac{\alpha+\lambda}{\alpha-\lambda}}$.
- $f_{\alpha,\lambda} = \frac{\Gamma(1+2i\lambda)}{\Gamma(1+i\lambda-i\alpha)}$ and $e^{2i\zeta(k)} = \frac{i(1+i\mu)}{(1-i\mu)} e^{2i\lambda \ln(2ka_0)}$.

Scattering Phase Shift

- The scattering phase shift is given by

$$\delta_\nu(k) = \arg[e^{-i\zeta(k)} + be^{i\zeta(k)}] - \alpha \ln(2kr) + \arg(f_{\alpha,\lambda}) \quad (10)$$

where $b = e^{-\pi\lambda} \mu \frac{f_{\alpha,-\lambda}}{f_{\alpha,\lambda}}$.

- We plot (10) ignoring the Coulomb tail term $-\alpha \ln(2kr)$.
- The plot shows that the phase shift depends on the topology through its dependence on n via ν . When the coupling α is deeper in the supercritical region, the phase shift is observed to have more number of kinks, which indicate the bound states.

Plot of Scattering Phase Shift

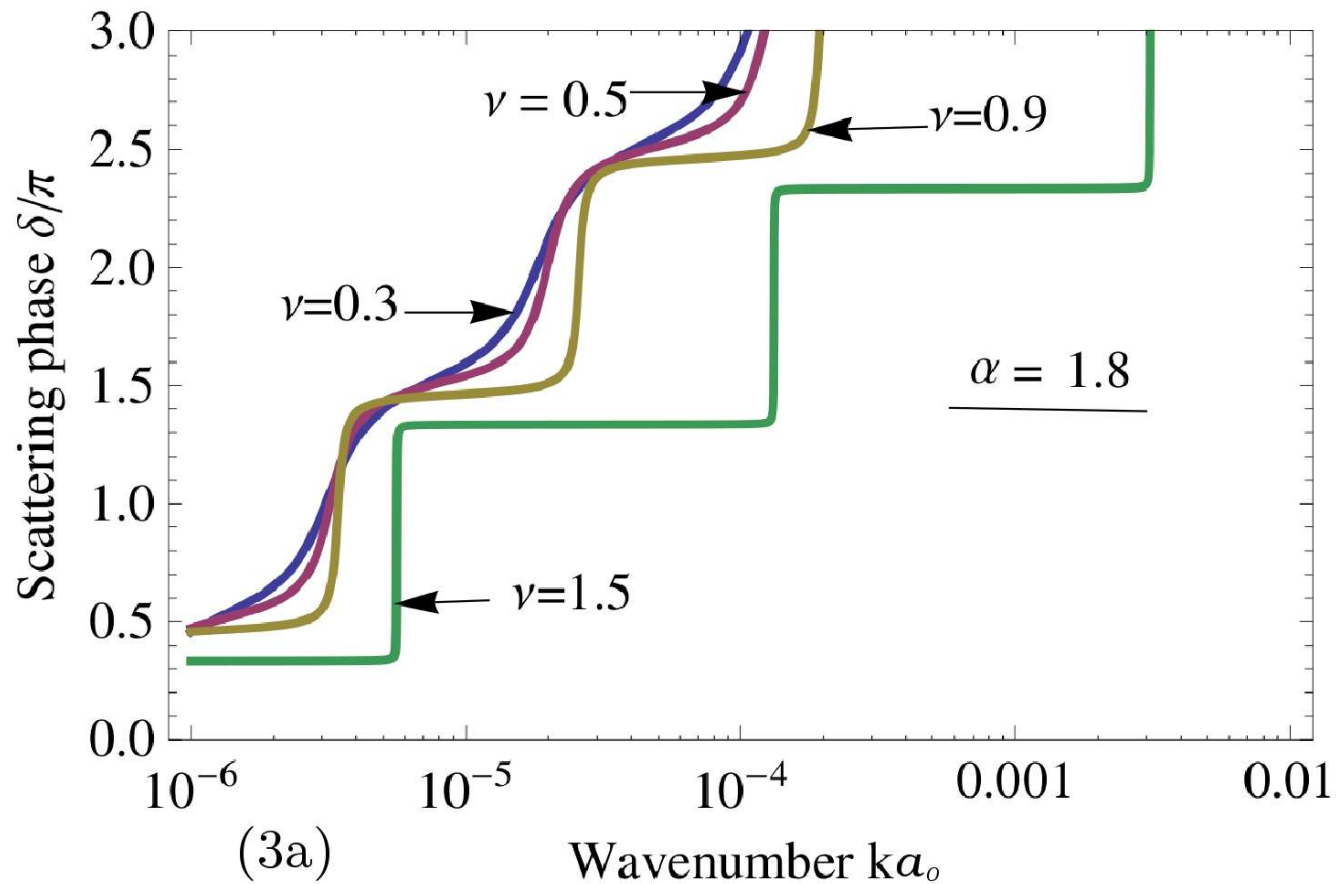


Figure 4: Dependence of scattering phase shift δ on wavenumber ka_0 for $\nu = 0.3, 0.5, 0.9, 1.5$ and $\alpha = 1.8$, ignoring the Coulomb tail term $-\alpha \ln(2kr)$. As the value of ν increases, the kinks in the phase shift become sharper, which indicates the dependence of the phase shift on the angle of the graphene cone.

Quasi-bound state Energy

- In gapless graphene we do not expect bound states due to **Klein tunneling**.
- In the supercritical regime, the system admits quasi-bound states whose spectrum is obtained from the zeroes of the S matrix in (9).
- The quasi-bound state energies are given by

$$E_p = -\frac{1}{2a_0} \exp \left[-\frac{p\pi}{\lambda} + i \left(\frac{1}{2\alpha} - \frac{\pi}{2} \right) \right], \quad (11)$$

where p is a positive integer.

Plot of Quasi-bound state Energy

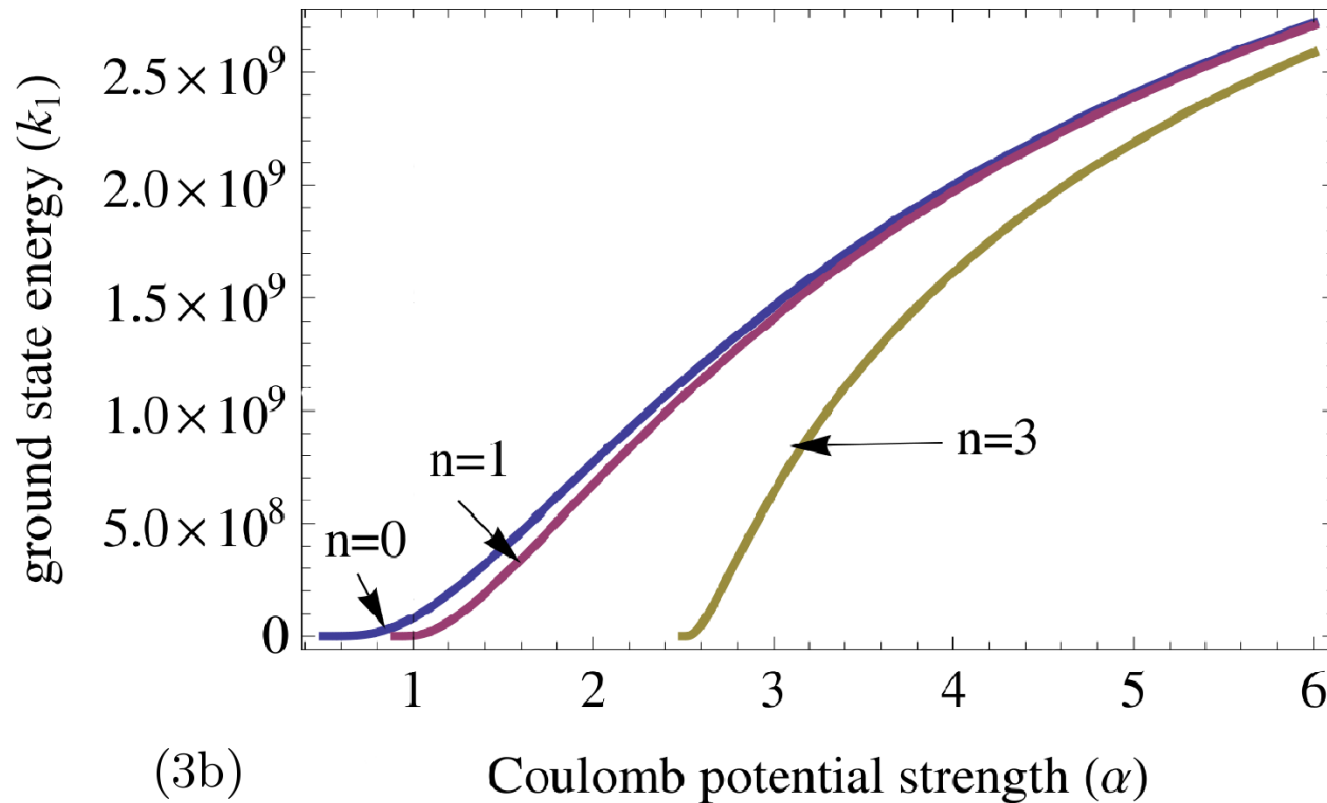


Figure 5: Dependence of ground state energy on the Coulomb potential strength for different angles of the graphene cone. We have considered $\nu = \frac{j + \frac{n}{4}}{1 - \frac{n}{6}}$ and $j = \frac{1}{2}$.

LDOS

Another interesting observable in this context is the LDOS. We have plotted the standing wave oscillations in LDOS $\rho(k, r)$ using

$$\rho(k, r) = \frac{4}{\pi \hbar v_F} \sum_j |\Psi^{(j)}(k, r)|^2, \quad (12)$$

where $\Psi^{(j)}(k, r)$ is the radial part of the Dirac spinor, for a given angular momentum channel j .

Plot of Standing Wave Oscillation in LDOS

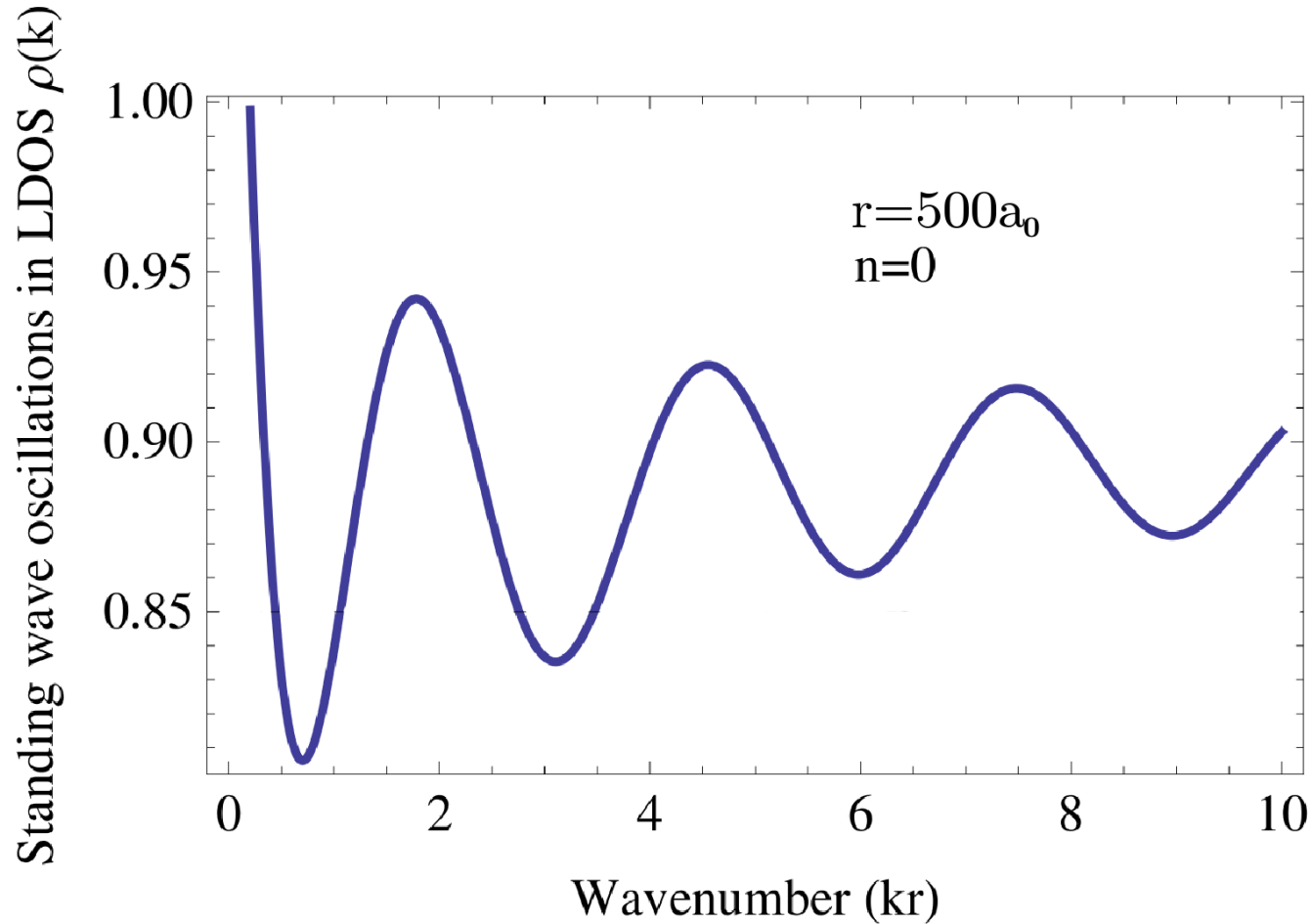


Figure 6: Energy dependence of LDOS in presence of a Coulomb potential for $n = 0$ and a particular value of r and with $j = \frac{1}{2}$ and $\alpha = 0.6$.

Plot of Standing Wave Oscillation in LDOS

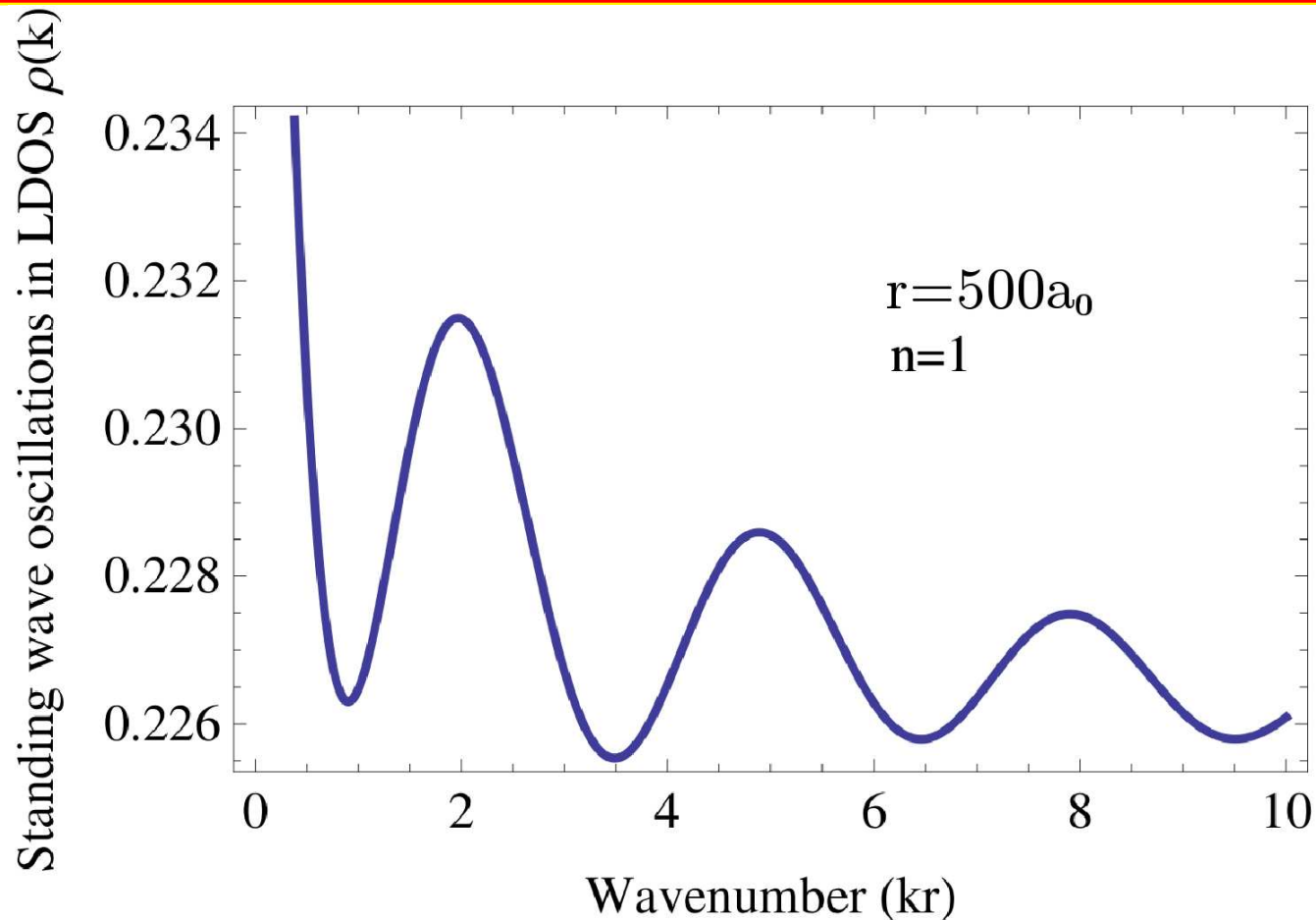


Figure 7: Energy dependence of LDOS in presence of a Coulomb potential for $n = 1$ and a particular value of r and with $j = \frac{1}{2}$ and $\alpha = 0.6$.

RG Flow of Charge Impurity Strength

- The real part of E_p in (11) diverges as the cutoff $a_0 \rightarrow 0$.
- To study the RG flow, we now promote the coupling constant α as a function of a_0 and demand that as $a_0 \rightarrow 0$, the energy for any fixed level p (say $p = 1$) remains independent of the cutoff.
- In the leading order, where α is only slightly above the critical coupling, this prescription gives the β -function as

$$\beta(\lambda) \sim -\lambda^2 + .. \quad (13)$$

- Thus we have an ultraviolet stable fixed point at $\lambda = 0$ or at $\alpha = \nu$. Hence, for any given value of n and j , the coupling α in the supercritical regime is driven to its critical value.

Conclusions

- The system of a graphene cone with an external Coulomb charge at its apex has been described by the combination of the Coulomb charge and a suitable magnetic flux tube passing through the apex.
- The above analysis has been done in the supercritical regime.
- The quantities of physical interest in this system include the scattering phase shifts, the LDOS and the quasi-bound state energies. We have shown that all these physical quantities depend explicitly on the number of sectors removed from a planar graphene to form the cone.
- The existence of the quasi-bound states indicates the possibility of the localization of the wavefunctions in the presence of a supercritical charge. Our analysis shows that the nature and extent of the localization depends on the spatial topology of the graphene sample.
- We have given qualitative arguments which shows that under the RG flow and for $\nu \neq 0$, the supercritical charge in the graphene cone tends to its critical value. If this argument can be extended for $\nu = 0$, for which the critical charge vanishes, that would lead to complete shielding of the external charge. This issue and the related electronic properties are currently under investigation.

THANK YOU